

On post-Newtonian orbits and the Galactic-center stars

Miguel Preto

*Astronomisches Rechen-Institut, Zentrum für Astronomie,
University of Heidelberg, D-69120 Heidelberg, Germany*

and

Prasenjit Saha

*Institute for Theoretical Physics, University of Zürich,
Winterthurerstrasse 190, CH-8057 Zürich, Switzerland*

ABSTRACT

Stars near the Galactic center reach a few percent of light speed during pericenter passage, which makes post-Newtonian effects potentially detectable. We formulate the orbit equations in Hamiltonian form such that the $O(v^2/c^2)$ and $O(v^3/c^3)$ post-Newtonian effects of the Kerr metric appear as a simple generalization of the Kepler problem. A related perturbative Hamiltonian applies to photon paths. We then derive a symplectic integrator with adaptive time-steps, for fast and accurate numerical calculation of post-Newtonian effects. Using this integrator, we explore relativistic effects. Taking the star S2 as an example, we find that general relativity would contribute tenths of mas in astrometry and tens of km s^{-1} in kinematics. (For eventual comparison with observations, redshift and time-delay contributions from the gravitational field on light paths will need to be calculated, but we do attempt these in the present paper.) The contribution from stars, gas, and dark matter in the Galactic center region is still poorly constrained observationally, but current models suggest that the resulting Newtonian perturbation on the orbits could plausibly be of the same order as the relativistic effects for stars with semi-major axes $\gtrsim 0.01$ pc (or 250 mas). Nevertheless, the known and distinctive *time dependence* of the relativistic perturbations may make it possible to disentangle and extract both effects from observations.

Subject headings: galaxy: center, relativity, stellar dynamics, methods: numerical

1. Introduction

The Galactic-center stars are a population of fast-moving stars in highly eccentric nearly Keplerian orbits around a compact mass — presumably a massive black hole (henceforth MBH) — of mass $\simeq 4 \times 10^6 M_\odot$ (Ghez et al. 2005; Ghez et al. 2008; Gillessen et al. 2009). Pericenter distance for some of these stars are inferred to be $< 10^4$ of the gravitational radius ($\simeq 3 \times 10^3$ in the case of S2) implying pericenter velocities of a few percent of light.

The high pericenter velocities inspire a search for general relativistic perturbations to Keplerian orbits. Jaroszynski (1998) and Fragile & Mathews (2000) suggested that the precession of the pericenter, which is an effect of $O(v^2)$ where v is the pericenter velocity in light units, would be observable. Interferometric instruments currently under development (see, for example, Eisenhauer et al. 2009) make this possibility more likely. If stars even further in are discovered, then $O(v^4)$ could become detectable from astrometry, leading to tests of no-hair theorems (Will 2008). Other consequences of general relativity may become accessible to spectroscopic observations. Zucker et al. (2006) note that the $O(v^2)$ effect of gravitational redshift may be within the reach of current instruments. Kannan & Saha (2009) suggest that the next generation of spectrographs may pick up even the $O(v^4)$ signature of frame dragging for the known Galactic-center stars.

To study the relativistic perturbations in detail, good methods for computing them numerically are highly desirable. In this paper we provide such a method.

Since geodesics in a Kerr metric are integrable (see, for example, chapter 7 of Chandrasekhar 1983), our problem may at first seem a trivial one. But the known integrability only puts the solution in terms of quadratures, it does not provide solutions in terms of elementary functions. The explicit forms given by Kraniotis (2007) for polar orbits, and the numerical methods given by Dexter & Agol (2009) for computing null geodesics give an idea of the complexity of the formally exact solutions. Moreover, even if one had the exact Kerr geodesics, one would need to perturb them for the Galactic-center stars, because of masses other than the black hole.

In this paper we take a different route. We go back to the Kerr metric and derive a post-Newtonian Hamiltonian, where relativistic effects appear as perturbations to Keplerian orbits and to which Newtonian perturbations due to other masses can be trivially added. Then we consider numerical algorithms designed for comets and other highly eccentric orbits in the solar system, and generalize them to work for post-Newtonian perturbations as well.

2. A post-Newtonian Hamiltonian

Geodesic equations in a given metric can be described in terms of a Lagrangian

$$L = \frac{1}{2} g_{\mu\nu} \frac{dx^\mu}{d\tau} \frac{dx^\nu}{d\tau}, \quad (1)$$

where τ is the affine parameter which, conveniently for us, can be identified with the star's proper time. Less common is the equivalent Hamiltonian form

$$H = \frac{1}{2} g^{\mu\nu} p_\mu p_\nu. \quad (2)$$

In fact H and L are equal, and conserved along geodesics. The above duality is simply a consequence of being quadratic.

We want to derive a post-Newtonian Hamiltonian for a test particle in a Kerr metric. To do this, we write the metric in Boyer-Lindquist coordinates, adopting $(-, +, +, +)$ for the signature of the metric and choosing units in which $G = c = 1$, as follows:

$$g_{\mu\nu} = \begin{pmatrix} -\left(1 - \frac{2\mu}{\Sigma}\right) & & & -\frac{2\mu\sigma}{\Sigma} r \sin\theta \\ & \frac{\Sigma}{\Delta} & & \\ & & \Sigma r^2 & \\ -\frac{2\mu\sigma}{\Sigma} r \sin\theta & & & \left(\Delta + \frac{2\mu}{\Sigma}(\Delta + 2\mu)\right) r^2 \sin^2\theta \end{pmatrix}. \quad (3)$$

Here we have defined

$$\mu = \frac{M}{r} \quad \sigma = \frac{s}{r} \sin\theta \quad \kappa = \frac{s}{r} \cos\theta \quad (4)$$

and

$$\Sigma \equiv 1 + \kappa^2 \quad \Delta \equiv 1 - 2\mu + \kappa^2 + \sigma^2, \quad (5)$$

where the dimensionless spin parameter $s \in [0, 1]$. The contravariant components are, as is not too difficult to verify by inverting the matrix, as follows:

$$g^{\mu\nu} = \begin{pmatrix} -\left(1 + \frac{2\mu}{\Sigma\Delta}(\Delta + 2\mu)\right) & & & -\frac{2\mu\sigma}{\Sigma\Delta} r \sin\theta \\ & \frac{\Delta}{\Sigma} & & \\ & & \frac{1}{\Sigma r^2} & \\ -\frac{2\mu\sigma}{\Sigma\Delta} r \sin\theta & & & \frac{1 - \sigma^2/\Delta}{\Sigma\Delta} r^2 \sin^2\theta \end{pmatrix}. \quad (6)$$

Expanding to second order in μ , σ , and κ we have

$$g^{\mu\nu} = \begin{pmatrix} -(1 + 2\mu + 4\mu^2) & & & -\frac{2\mu\sigma}{r \sin \theta} \\ & 1 - 2\mu + \sigma^2 & & \\ & & \frac{1 - \kappa^2}{r^2} & \\ -\frac{2\mu\sigma}{r \sin \theta} & & & \frac{1}{r^2 \sin^2 \theta} \end{pmatrix}. \quad (7)$$

Now we proceed to consider the Hamiltonian. For simplicity, we put $M = 1$, which just means we are measuring r in units of the gravitational radius, GM/c^2 . To consider dynamics at large- r we replace ¹

$$r \rightarrow \epsilon^{-2}r. \quad (8)$$

The Hamiltonian will now have two regimes.

In the low-velocity regime we require the velocity terms to be $O(\epsilon)$. This is achieved with the substitutions

$$p_r \rightarrow \epsilon p_r \quad p_\theta \rightarrow \epsilon^{-1}p_\theta \quad p_\phi \rightarrow \epsilon^{-1}p_\phi \quad (9)$$

which gives

$$H = -\frac{p_t^2}{2} + \left(\frac{p_r^2}{2} + \frac{p_\theta^2}{2r^2} + \frac{p_\phi^2}{2r^2 \sin^2 \theta} - \frac{p_t^2}{r} \right) \epsilon^2 - \left(\frac{2p_t^2}{r^2} + \frac{p_r^2}{r} \right) \epsilon^4 - \frac{2sp_t p_\phi}{r^3} \epsilon^5 + O(\epsilon^6). \quad (10)$$

At zeroth order, a test particle just stays still. At $O(\epsilon^2)$ it follows Newtonian dynamics. Relativistic effects appear at $O(\epsilon^4)$, while frame-dragging appears at $O(\epsilon^5)$. But note that the kinematic effects themselves are at one order of ϵ lower: thus Newtonian velocities are $O(\epsilon)$, Schwarzschild perturbations to the velocities are $O(\epsilon^3)$, while the frame-dragging perturbation to velocity is $O(\epsilon^4)$. Gravitational radiation is a higher-order effect which we disregard here, and in any case the timescale for orbital decay of the S2 star due to radiation reaction is longer than a Hubble time.

In the light-velocity regime we require the velocity terms to be $O(1)$. Thus we replace

$$p_\theta \rightarrow \epsilon^{-2}p_\theta \quad p_\phi \rightarrow \epsilon^{-2}p_\phi \quad (11)$$

which gives

$$H = -\frac{p_t^2}{2} + \frac{p_r^2}{2} + \frac{p_\theta^2}{2r^2} + \frac{p_\phi^2}{2r^2 \sin^2 \theta} - \left(\frac{p_t^2}{r} + \frac{p_r^2}{r} \right) \epsilon^2 + \left(\frac{2p_t^2}{r^2} - \frac{s^2 \sin^2 \theta}{2r^2} p_r^2 + \frac{s^2 \cos^2 \theta}{2r^4} p_\theta^2 + \frac{2sp_t p_\phi}{r^3} \right) \epsilon^4 + O(\epsilon^6). \quad (12)$$

¹Here ϵ is just a label for keeping track of orders. Numerically $\epsilon = 1$.

At zeroth order, null geodesics just move in straight lines. The leading perturbation is at $O(\epsilon^2)$.

The Hamiltonian (10) is the approximate Hamiltonian we will use, but we can simplify its form with some variable changes. First, we set $p_t = -1$, which we are free to do since the Hamiltonian is autonomous. This merely sets units for the affine parameter such that $dt/d\tau = -1$ in the large- r limit, and has no physical significance. Then, we change from r, θ, ϕ to x, y, z . Completing the canonical transformation, we have

$$p_r = \frac{\mathbf{x} \cdot \mathbf{p}}{r}, \quad p_\phi = (\mathbf{x} \times \mathbf{p})_z, \quad (13)$$

and hence

$$p_r^2 + \frac{p_\theta^2}{r^2} + \frac{p_\phi^2}{r^2 \sin^2 \theta} = \mathbf{p}^2. \quad (14)$$

The post-Newtonian Hamiltonian (10) then becomes

$$H = H_{\text{Kep}} + H_{\text{S}} + H_{\text{LT}}, \quad (15)$$

where

$$\begin{aligned} H_{\text{Kep}} &= \frac{\mathbf{p}^2}{2} - \frac{1}{r}, \\ H_{\text{S}} &= -\frac{2}{r^2} - \frac{(\mathbf{x} \cdot \mathbf{p})^2}{r^3}, \\ H_{\text{LT}} &= 2 \frac{\mathbf{s} \cdot \mathbf{x} \times \mathbf{p}}{r^3}. \end{aligned} \quad (16)$$

There is a separate equation for t

$$\dot{t} = 1 + \frac{2}{r} + \frac{4}{r^2} - \frac{2sp_\phi}{r^3}. \quad (17)$$

3. An adaptive-timestep symplectic integrator

The post-Newtonian orbit equations can be integrated numerically by any general-purpose method for ordinary differential equations. Another option is to use an N -body simulation code for dense stellar systems, with post-Newtonian terms added (Mikkola & Merritt 2008). A computationally more efficient strategy, however, would be an integration algorithm that takes advantage of the above formulation of relativistic effects as small perturbation to a Kepler Hamiltonian. We now design such an integration algorithm, based on recent work on cometary orbits, which are also highly eccentric orbits that experience interesting perturbations around pericenter passage.

When integrating Hamiltonian systems numerically, it is a common practice to impose the condition that the numerical solution has (to machine precision) the symmetry properties of Hamiltonian flow. Integration algorithms with this property are known as symplectic integrators. A simple but important example is generalized leapfrog. Suppose we have a Hamiltonian that is the sum of two parts $H = H_A + H_B$ where H_A and H_B are individually easy or trivial to integrate. Generalized leapfrog evolves under H for a time step $\Delta\tau$ as follows.

1. Evolve under H_A for time $\frac{1}{2}\Delta\tau$.
2. Evolve under H_B for time $\Delta\tau$.
3. Reiterate step 1.

If $H = \frac{1}{2}\mathbf{p}^2 + V(\mathbf{x})$ the above becomes the classical leapfrog integrator. It turns out (see, for example, Forest & Ruth 1990) that generalized leapfrog amounts to evolving under a “surrogate” Hamiltonian

$$H_A + H_B + \left(\frac{1}{12}\{H_A, H_B\}, H_B \right) + \frac{1}{24}\{H_A, H_B\}, H_A \Delta\tau^2 + O(\Delta\tau^4). \quad (18)$$

The nested Poisson brackets amount to a Hamiltonian expression for the error, which is manifestly second order. Higher-order extensions are possible (Forest & Ruth 1990; Yoshida 1990; Laskar & Robutel 2001) but in practice second-order is the most used. If one of H_A or H_B is much smaller than the other, the error Hamiltonian will be correspondingly small. Wisdom & Holman (1991) and independently Kinoshita et al. (1991) proposed integrators for planetary orbits where H_A is the integrable Kepler Hamiltonian and H_B encapsulates the perturbations. For planetary orbits, the low order of generalized leapfrog becomes an advantage in that the steps can be made comparatively large (≈ 10 steps per orbit) and still provide high accuracy. Further refinements are possible, such as perturbative pre-processing of the initial conditions (Saha & Tremaine 1992) or perturbative post-processing of the results (Wisdom et al. 1996), but the original Wisdom-Holman scheme is the most common choice for long-term solar-system orbit integrations.

Another kind of symplectic integrator, also second order, is the implicit midpoint method, due to Feng (1986). This can be written as a simple discretization of Hamilton’s equations

$$\Delta\mathbf{x} = \left(\frac{\partial H}{\partial \mathbf{p}} \right) \Delta\tau \quad \Delta\mathbf{p} = - \left(\frac{\partial H}{\partial \mathbf{x}} \right) \Delta\tau \quad (19)$$

with the derivatives are evaluated at the midpoint

$$\left(\mathbf{p} + \frac{1}{2}\Delta\mathbf{p}, \mathbf{x} + \frac{1}{2}\Delta\mathbf{x} \right). \quad (20)$$

It is essential for $\Delta\mathbf{x}, \Delta\mathbf{p}$ to be consistent between (19) and (20) to high accuracy (preferably machine precision), otherwise the symplectic property is lost. Hence, the implicit midpoint method requires iteration. But it requires no splitting of the Hamiltonian, and hence is very useful when generalized leapfrog is inapplicable. A surrogate Hamiltonian for the implicit midpoint integrator is derived in Saha et al. (1997).

Combining the two above ingredients, a possible integration method for the Galactic-center stars would be a generalized leapfrog with $H_A = H_{\text{Kep}}$ and $H_B = H_S + H_{\text{LT}} + V_{\text{Gal}}$, with an exact Kepler solution used for the former, and implicit midpoint used for the latter. In fact, neither of the separate integrations under H_A and H_B needs to be exact. As long as they are symplectic and second-order, the surrogate Hamiltonian (18) will apply.

For low eccentricities, an integrator as above would be very efficient. When we consider Galactic-center stars (or comets) however, we run into the major limitation of generalized leapfrog: the stepsize $\Delta\tau$ must remain fixed, otherwise the integrator is no longer symplectic. Yet for $e \approx 0.9$, the very small $\Delta\tau$ needed at pericenter becomes hopelessly expensive if used throughout an orbit. Adaptive time-stepping is needed.

The key to adaptive time-stepping is to transform from τ to a new independent variable (say s) which somehow implements the desired stretching and shrinking of the stepsize without breaking the symplectic property. Mikkola (1997) provided the first example, showing how a simple modification of the Wisdom-Holman algorithm effectively creates the variable s with $d\tau = r ds$. Then Preto & Tremaine (1999) and independently Mikkola & Tanikawa (1999) formulated, for a Hamiltonian $\frac{1}{2}\mathbf{p}^2 + V(\mathbf{x})$, a time transformation with $d\tau = -ds/V(\mathbf{x})$. As a by-product, this work produced a leapfrog for H_{Kep} that is symplectic and in fact recovers the exact answer except for a very small phase error, but is computationally much simpler than the exact solution. Mikkola & Aarseth (2002) then generalized these ideas to make the time-transformation completely adaptive, though not in a Hamiltonian formulation, so it was not manifestly symplectic. Later, Emel’yanenko (2007) supplied an elegant Hamiltonian derivation of adaptive stepsize.

Based on all the above, we now develop our integrations algorithm. The derivation basically follows Emel’yanenko (2007) but is written with a view to application to post-Newtonian orbits.

Let us enhance the phase space (\mathbf{x}, \mathbf{p}) . We now treat τ as an additional coordinate, with a new variable Φ being its conjugate momentum, and the new independent variable s . In this enhanced phase space, consider the Hamiltonian

$$F(\mathbf{x}, \tau, \mathbf{p}, \Phi) = \frac{H - k}{\Phi} + \ln\left(\frac{\Phi}{\varphi(\tau)}\right), \quad (21)$$

where $\varphi(\tau)$ is a known function and k is a constant. Hamilton's equations for F are

$$\frac{d\mathbf{x}}{ds} = \frac{1}{\Phi} \frac{\partial H}{\partial \mathbf{p}} \quad \frac{d\mathbf{p}}{ds} = -\frac{1}{\Phi} \frac{\partial H}{\partial \mathbf{x}}, \quad (22)$$

together with

$$\frac{d\Phi}{ds} = \frac{d}{d\tau} \ln \varphi \quad (23)$$

and

$$\frac{d\tau}{ds} = -\frac{H - k}{\Phi^2} + \frac{1}{\Phi}. \quad (24)$$

Moreover, F will be conserved.

Suppose at some s we have $H = k$. Combining the two previous equations, we infer that at this point

$$\frac{d}{d\tau} \ln \Phi = \frac{d}{d\tau} \ln \varphi. \quad (25)$$

Thus, in the neighborhood of this point, Φ/φ will be constant, and hence $H - k$ will remain zero. In other words, if

$$\frac{d\tau}{ds} = \frac{1}{\Phi}, \quad (26)$$

holds initially, it will continue to hold. The interpretation is the original Hamiltonian equations with a rescaled variables $ds = \Phi d\tau$.

Now the cunning part: we consider $\varphi(\tau)$ as $\varphi(\mathbf{x}, \mathbf{p})$ where \mathbf{x}, \mathbf{p} are functions of τ , and replace $d\varphi/d\tau$ by the convective derivative. We have:

$$\frac{d\Phi}{ds} = \left(\frac{d\mathbf{x}}{d\tau} \cdot \frac{\partial}{\partial \mathbf{x}} + \frac{d\mathbf{p}}{d\tau} \cdot \frac{\partial}{\partial \mathbf{p}} \right) \ln \varphi(\mathbf{x}, \mathbf{p}) \quad (27)$$

With the above ingredients in hand, we proceed to write a leapfrog for F in the variable s :

1. Holding \mathbf{x}, \mathbf{p} constant, advance Φ using (27) over $\Delta s = \frac{1}{2}$. This amounts to evolution under a Hamiltonian $-\ln \varphi$.
2. Holding Φ constant, evolve \mathbf{x}, \mathbf{p} under H/Φ for $\Delta s = 1$, and advance τ by 1. This amounts to evolution under a Hamiltonian $(H - k)/\Phi + \ln \Phi$.
3. Reiterate step 1.

In the present work, step 2 above consists of a generalized leapfrog with the main Hamiltonian split into Keplerian, post-Newtonian, and external potential parts. We also have two minor simplifications: (i) we assume φ depends only on \mathbf{x} , and (ii) we disregard the evolution of τ . The simplified treatment of time is fine for our test particle integrations, but for an N -body formulation, the time equation needs to be treated with special care, and the form $d\tau = ds/\Phi$, associated with the new pair of conjugate variables (τ, Φ) presents several advantages.

The algorithm is as follows.

1. Advance Φ by $\frac{1}{2}(\partial H/\partial \mathbf{p}) \cdot \nabla(\ln \varphi)$.
2. Evolve \mathbf{x}, \mathbf{p} under H_{Kep} for $\Delta\tau = 1/(2\Phi)$, using the algorithmic regularization scheme of Preto & Tremaine (1999).
3. Evolve \mathbf{x}, \mathbf{p} under $H_{\text{S}} + H_{\text{LT}} + V_{\text{Gal}}$ for $\Delta\tau = 1/\Phi$, using the implicit midpoint method. For the small post-Newtonian contributions of interest for this paper, this implicit scheme converges to machine precision in two or three iterations.
4. Reiterate step 2.
5. Reiterate step 1.

The following comments about the integrator are worth making. First, with the simplest choice $\varphi \propto 1/r$, we obtain an adaptive, symplectic integrator to integrate eccentric weakly-perturbed Keplerian orbits — including non-separable post-Newtonian perturbations. This integrator is easy to implement, and it is free from the instability found Rauch & Holman (1999) in fixed-stepsize integration of highly eccentric orbits. Second, with the apparently innocuous modification of the time transformation to $d\tau = ds/\Phi$, the Keplerian part becomes trivial to integrate, since Φ is kept constant while the (cartesian) coordinates are advanced. This is very advantageous for a N -body implementation with individual time steps, where particle synchronization requires numerous Kepler drifts. Third, being a symplectic integrator, errors in the longitudes grow only linearly with time and, for spherical perturbations, angular momentum is conserved to machine precision. This is clearly a most desirable property — in particular, in dynamical problems for which long term integrations with accurate tracking of all phase angles are required, *e.g.*, resonant relaxation and related effects (Gürkan & Hopman 2007; Madigan et al. 2009; Perets et al. 2009). Fourth, as pointed out already by Emel’yanenko (2007), the freedom to choose the functional form of φ provides an additional degree of freedom that can be explored in order to resolve close encounters without breaking symplecticity. Fifth, this integrator and the post-Newtonian approximation presented in this work are very well suited to be included in orbital fitting

routines of the Galactic-center stars (Weinberg et al. 2005; Gillessen et al. 2009). Sixth, this symplectic integrator is also ideally suited for implementation in view of N -body modelling of gravitational wave sources, *e.g.* extreme mass ratio inspirals, which are of great interest for LISA (Laser Interferometer Space Antenna).

4. Numerical results

As an illustration, we consider perturbations of the orbit with Keplerian elements

$$a = 2.4 \times 10^4 \quad e = 0.88 \quad I = 135.25^\circ \quad \Omega = -134.71^\circ \quad \omega = 63.56^\circ \quad (28)$$

which are approximately the measured values for S2 (Gillessen et al. 2009). Note that a is in units of the gravitational radius $GM/c^2 \simeq 5 \times 10^6$ km or $\simeq 4\mu\text{as}$ on the sky. We assume the spin is unity (maximal) and directed along $+z$.

We begin by verifying that the integrator is indeed second order and that the phase error grows linearly with time. From Figure 1 we see that the maximum error in H is proportional to $\Phi^{-2}(0)$, where $1/\Phi(0)$ is the initial stepsize, and that the error in pericenter angle is proportional to the number of orbits (*i.e.* it is linear rather quadratic). In order to evaluate this error we adopt the expressions for the shift of pericenter due to a Schwarzschild black hole up to 2^{nd} order (Weinberg 1972; Nucita et al. 2007) and the 1^{st} order contribution from the spin (Kannan & Saha 2009):

$$\begin{aligned} \Delta\omega_s &= \frac{6\pi}{a(1-e^2)} + \frac{3\pi(18+e^2)}{2a^2(1-e^2)^2} \\ \Delta\omega_{fd} &= -\frac{12\pi s \cos I}{a^{3/2}(1-e^2)^{3/2}}. \end{aligned} \quad (29)$$

The observable orbit, that is to say, the sky position and redshift as a function of observer time, depends also on the light path from the star to the observer. There are two types of effects.

1. The sky position of the star will be slightly shifted by gravitational lensing. The maximum lensing displacement is the Einstein radius R_E . Since for Galactic-Center stars, the lens-source distance D_{LS} is much smaller than the observer-source and lens-source distances, the usual expression for R_E simplifies to

$$R_E = 2\sqrt{D_{LS}} \quad (30)$$

in units of the gravitational radius, and D_{LS} will be of order a .

2. Then there is the redshift, and the Rømer effect, which can be considered as the redshift integrated along the orbit. The $O(\epsilon)$ contribution to the redshift is classical. Special relativity and the time part of the metric both contribute to the redshift at $O(\epsilon^2)$, while space curvature contributes at $O(\epsilon^3)$.

We do not include all these effects in this paper, leaving it for future work, because at this stage our aim is to gain some insight into the size of relativistic effects rather than calculate observables precisely. However, following Zucker et al. (2006), we include the $O(v^2)$ effects due to gravitational time dilation when we estimate the perturbations on the radial velocities.

Having chosen the orbital elements, we start the star at apocenter and integrate the orbit under the Hamiltonian (15) to the next apocenter passage. Figure 2 shows a , ω , and Ω along the orbit, as a function of the mean anomaly, which is a surrogate for time. The range -180 to 180 in the mean anomaly corresponds to a Keplerian orbit going from apocenter to apocenter. In this paper we always compare perturbed and unperturbed orbits for the same value of mean anomaly, not necessarily the same value of time. If time is taken as the independent variable, an artificial secular drift would appear, because the perturbed orbit has a slightly different orbital period. The other two Keplerian elements are not shown here, because I and $a(1 - e^2)$ are constant as a consequence of the conservation of total angular momentum, which the symplectic integrator reproduces to roundoff error.

From Figure 2, one easily verifies the well-known leading-order expressions

$$\Delta\omega = \frac{6\pi}{a(1 - e^2)} \quad (31)$$

for the pericenter precession and

$$\Delta\Omega = -\frac{8\pi \cos I}{(a(1 - e^2))^{3/2}} \quad (32)$$

for Lense-Thirring node precession. The maximum change in a can be estimated as follows. We start by noting from the inspection of (16) that the leading post-Newtonian perturbation is

$$\Delta H = \frac{2}{r^2} \quad (33)$$

at both pericenter and apocenter. Since at these points $r = a(1 \pm e)$ we have

$$\Delta H_{\text{peri}} - \Delta H_{\text{apo}} = \frac{8e}{a^2(1 - e^2)^2} \quad (34)$$

For the unperturbed Hamiltonian $H = -1/(2a)$ hence $\Delta H \simeq \Delta a/(2a^2)$ from which it follows

$$\Delta a = \frac{16e}{(1 - e^2)^2} \quad (35)$$

Using similar arguments, or dimensional analysis, one easily derives that the effects of a perturbation

$$\Delta H \sim r^{-n} \quad (36)$$

scale as follows.

$$\begin{aligned} \text{astrometric} \quad \Delta l, \Delta b &\sim a^{2-n} \\ \text{kinematic} \quad \Delta v &\sim a^{\frac{1}{2}-n} \\ \text{precession} \quad \Delta\omega, \text{ etc} &\sim a^{1-n} \end{aligned} \quad (37)$$

Post-Newtonian effects have $n = 2$ (Schwarzschild) or $n = 3$ (Lense-Thirring). Thus, the astrometric effect of Schwarzschild perturbations is independent of a to leading order, while other post-Newtonian effects get stronger as orbits get smaller. Relativistic prograde precession would seem easier to measure at larger distances, but that is not the case since the orbital period increases as $a^{3/2}$. On the other hand, Galactic perturbations from other masses than the black hole would have $n < 1$, and hence get weaker as orbits get smaller.

The form and strength of Newtonian Galactic perturbations, due to other stars, gas, and dark matter, are still poorly constrained at present. Observations aimed at measuring post-Newtonian effects would need to fit the local Galactic potential as well. Stars, however, are expected to be the dominant component of the extended galactic mass distribution near the central MBH. From observations, the stellar distribution around the MBH is best approximated by a double power-law density profile, with a (somewhat uncertain) break radius that may range from $r_b \sim 0.1 - 0.2$ pc up to $r \sim \text{few} \times 1\text{pc}$ (Schödel et al. 2007, 2009). This translates into a single power-law model $\rho(r) = \rho_0(r/r_0)^{-\gamma}$ throughout the whole region of special interest for us, $r \lesssim 0.01\text{pc}$. Therefore, we adopt the following gravitational potential V_{Gal}

$$V_{\text{Gal}} = \begin{cases} \frac{4\pi}{(3-\gamma)(2-\gamma)} \rho_0 r_0^\gamma r^{2-\gamma} = \frac{M_*(r_0)}{(2-\gamma)r_0} \left(\frac{r}{r_0}\right)^{2-\gamma}, & \gamma \neq 2, \\ 4\pi \rho_0 r_0^2 \ln\left(\frac{r}{r_0}\right) = \frac{(3-\gamma)M_*(r_0)}{r_0} \ln\left(\frac{r}{r_0}\right), & \gamma = 2, \end{cases} \quad (38)$$

where $M_*(r_0)$ is the total stellar mass within the radius r_0 . We will adopt $r_0 = 0.01\text{pc}$ in this paper.²

In the absence of definite observational measurements, and in order to chose the values for the slope γ and for the normalization of the mass distribution, we have to appeal to

²It is easy to see that $n = \gamma - 2$, so that $1/2 \leq \gamma < 3$ implies $-3/2 \leq n < 1/2$ in (36) and (37).

stellar dynamical theory. The relaxation time in the Milky Way’s nucleus is $T_R \sim O(1\text{Gyr})$ and therefore old stellar populations may have had enough time to reach a relaxed steady-state. Mass segregation around a MBH leads to steeper profiles for heavy stars (*e.g.* compact remnants such stellar black holes) than for light stars (Bahcall & Wolf 1977). Recent Fokker-Planck and N -body studies (Alexander & Hopman 2009; Preto & Amaro-Seoane 2009) show that mass segregation is indeed a generic and robust property of the relaxed populations around a MBH; furthermore, it is stronger than expected according to Bahcall & Wolf, and leads to power-law density profiles with slopes such as $\gamma_{\text{heavy}} \sim 1.8-2.3$ and $\gamma_{\text{light}} \sim 1.0-1.6$. According to the latter studies, the total amount of stellar mass packed inside $r_0 = 0.01\text{pc}$ is $M_*(r_0) \sim \alpha \times 2 \times 10^3 M_\odot$, where $\alpha = O(1)$. Therefore, in our numerical tests, we will adopt $\gamma = 1.5, 2.1$ and a normalization for the total stellar mass $M_*(r_0) = 2 \times 10^{3-4} M_\odot$. This leads to circular velocities, induced by stellar mass alone, of order 20–50 km/s. Current observational constraints on the mass normalization are still roughly one or two orders of magnitude above of these values, whereas γ is still very weakly constrained (Ghez et al. 2008; Gillessen et al. 2009).

Figures 3 and 4 illustrate astrometric perturbations from the relativistic terms and from the local Galactic model (38). Not surprisingly, for an orbit with semi-major axis a the galaxy’s perturbation effects are $\propto M_*(a)$. For the adopted parameters, the cusp slope has only a weak effect but it is noticeable; furthermore, the galaxy’s perturbations are also stronger for steeper cusps. Given the model adopted for the stellar cluster, the cumulative mass distribution is $M(r) = M_*(r_0)(r/r_0)^{3-\gamma}$, so when the slope γ changes by an amount $\Delta\gamma$, the total mass within a (orbital semi-major axis) changes by

$$\Delta M(a) = M_*(r_0) \left[\left(\frac{a}{r_0} \right)^{3-\gamma-\Delta\gamma} - \left(\frac{a}{r_0} \right)^{3-\gamma} \right]. \quad (39)$$

Therefore, increasing $\gamma = 1.5$ to 2.1 leads to a mass increment within a , $\Delta M_*(< a) \sim 0.19 M_*(a) \sim 3.8 \times 10^3 M_\odot$. Therefore a larger proper motion obtains which is, to first order, given by $\Delta l_{2.1} \sim \Delta l_{1.5} + \Delta l_{1.5} \times \Delta M(a) \sim 0.89 \text{ mas}$. The agreement with the plots in the two bottom panels of Figure 4 is very good. Figure 4 also shows that the small difference (for an S2-like orbit) between the purely relativistic perturbation and the combined relativistic plus Galactic perturbation is smaller than astrometric capabilities — even in the case when the extended stellar cluster is relatively massive.

Figure 5 shows the kinematic effect of relativistic and Galactic perturbations. As in the previous figures, the perturbations are shown as a function of mean anomaly. It can be seen that the relativistic kinematic perturbation on a S2-like star is strong enough to be detected by current instruments, for which $\delta v \sim 10 \text{ km/s}$. This is not the stronger case as the S14 star has a closer pericenter passage and thus suffers a stronger (by a factor of ~ 5) kinematic

perturbation.

In summary, three more things are evident from these figures that are worth commenting on.

- For most of the known S-stars, the Galactic perturbations could be comparable to the relativistic effects, and even rather similar in time dependence. Perturbations on S2 and S14 are, however, essentially dominated by relativistic effects. (Relativistic perturbations could dominate even more in stars further in, if such stars are discovered; this, combined with shorter periods, would make detecting the signature of the relativistic effects much neater.) It may be hoped, however, that even for the already-discovered stars, that the known and very specific form of the relativistic effects could enable them to be extracted, but it remains to be demonstrated.
- Kinematics perturbations are concentrated near pericenter passage, whereas astrometric perturbations are of the same order throughout the orbit. For highly eccentric orbits, the the astrometric perturbation Δl has two different origins: near pericenter, Δl is due to Δv , which shifts the phase of the orbit; near apocenter, Δl comes precession $\Delta\omega$, amplified by the lever arm of the orbit.
- Although the speed is maximal at pericenter, the kinematic perturbation is maximal (and can be much greater) at a phase before or after.

5. Comparison with other post-Newtonian formulations

In computing the preceding numerical results, we have made some non-trivial choices of convention.

1. We have worked in what may be called be the Boyer-Lindquist gauge, which for zero spin reduces to the standard gauge of the Schwarzschild spacetime.
2. Our independent variable is the affine parameter, which is proportional to the proper time.
3. Our kinematic variables are the canonical momenta, and not derivatives of the coordinates. In particular, when computing Keplerian elements, we have fed momentum and not velocity values into the classical formulas.

Different choices can lead to some surprising differences in the results. Of course, observable quantities must not change. But for abstract quantities such as the instantaneous a , even

the sign of the post-Newtonian effect can switch. We now explain how to convert to other conventions, considering for simplicity only the leading order Schwarzschild effects.

For a weak-field Schwarzschild spacetime, the most common gauge choice is the harmonic form, where the metric is

$$ds^2 = - \left(1 - \frac{2}{r} + \frac{2}{r^2} \right) dt^2 + \left(1 + \frac{2}{r} \right) d\mathbf{x}^2. \quad (40)$$

Working out $\frac{1}{2}g^{\mu\nu}$ we readily derive the Hamiltonian

$$H = -\frac{1}{2} \left(1 + \frac{2}{r}\epsilon^2 + \frac{2}{r^2}\epsilon^4 \right) p_t^2 + \frac{1}{2} \left(\epsilon^2 - \frac{2}{r}\epsilon^4 \right) \mathbf{p}^2 + O(\epsilon^6). \quad (41)$$

with ϵ labeling orders as before, through the replacements

$$r \rightarrow \epsilon^{-2}r \quad \mathbf{p} \rightarrow \epsilon \mathbf{p}. \quad (42)$$

Since there is no explicit dependence on t , the conjugate momentum p_t will be constant. As before, the initial value of p_t just sets the units of the affine parameter τ , but if we set

$$p_t = 1 + \left(\frac{\mathbf{p}^2}{2} - \frac{1}{r} \right) \epsilon^2 + \left(\frac{1}{2r^2} - \frac{3\mathbf{p}^2}{2r} - \frac{\mathbf{p}^4}{8} \right) \epsilon^4 \quad (43)$$

initially then $H = -\frac{1}{2} + O(\epsilon^6)$, and the affine parameter will equal the proper time along the orbit, to the given order.

As an aside, in Hamiltonian dynamics there is another possible interpretation of (43): we can take the function $p_t(\mathbf{x}, \mathbf{p})$ as a Hamiltonian in its own right, having three degrees of freedom and t as the independent variable. Saha & Tremaine (1994) used this Hamiltonian to incorporate the leading-order post-Newtonian effects into a symplectic algorithm for long-term integration of planetary orbits.

Considering now the coordinate velocity $\mathbf{v} \equiv d\mathbf{x}/dt$ we have

$$\epsilon \mathbf{v} = \left(\frac{dt}{d\tau} \right)^{-1} \left(\frac{d\mathbf{x}}{d\tau} \right) = \left(\frac{\partial H}{\partial p_t} \right)^{-1} \left(\frac{\partial H}{\partial(\epsilon \mathbf{p})} \right) \quad (44)$$

which for the Hamiltonian (41) gives

$$\mathbf{v} = p_t^{-1} \left(1 + \frac{2}{r}\epsilon^2 \right)^{-1} \left(1 - \frac{2}{r}\epsilon^2 \right) \mathbf{p} + O(\epsilon^4). \quad (45)$$

Substituting from (43) and rearranging, we have

$$\mathbf{v} = \left(1 - \left(\frac{\mathbf{p}^2}{2} + \frac{3}{r} \right) \epsilon^2 \right) \mathbf{p} + O(\epsilon^4). \quad (46)$$

Thus while $\mathbf{x} \times \mathbf{p}$ is a constant of motion, in $\mathbf{x} \times \mathbf{v}$ the modulation (46) appears (cf. the leading term in Equation 4.9 in Blanchet & Iyer 2003, taking their $\nu = 0$ in the test particle limit).

As noted above, for the main results of this paper, we have computed orbital elements using the “momentum convention”, as

$$-\frac{1}{2a} = \frac{\mathbf{p}^2}{2} - \frac{1}{r} \quad a(1 - e^2) = |\mathbf{x} \times \mathbf{p}|^2 \quad (47)$$

and so on. On the other hand, if the “velocity convention”

$$-\frac{1}{2a} = \frac{\mathbf{v}^2}{2} - \frac{1}{r} \quad a(1 - e^2) = |\mathbf{x} \times \mathbf{v}|^2 \quad (48)$$

is adopted instead, it follows from (46) that the orbital elements can change at $O(\epsilon^2)$.

Figure 6 shows the perturbations of the orbital elements (as in the top two panels of Figure 2), but now computed by following the “velocity convention”. It can be seen that the semimajor axis perturbation changes its sign; while ω now shows a small oscillation around pericenter.

6. Conclusions

The prospect of detecting general relativistic effects in the S-stars near the Galactic center has recently aroused interest. To help gain more insight into these small but exciting effects, we have derived a simple formulation for the orbit equations and an algorithm for numerically integrating them, in which the post-Newtonian dynamics appears clearly as perturbations of the Kepler problem, and then examined the size of the perturbations.

The post-Newtonian Hamiltonian is (10) or equivalently (15-16). These look like and are fairly simple generalizations of the Keplerian Hamiltonian, the main difference being that time is a coordinate and the affine parameter is an independent variable. For numerical integration we adapt the variable-timestep symplectic integrators recently developed for cometary or other highly eccentric orbits in the solar system.

For photons a somewhat different approximation applies than for (comparatively) slow-moving stars, and we derive the Hamiltonian (12). It leads to gravitational redshift and related effects, but we leave the computation of these for future work.

With the orbit integrator we proceed to compute the effects of the post-Newtonian terms on the orbital elements, sky position, and kinematics, taking the orbit of S2 as an example.

For S2, general relativity implies an astrometric effect of tenths of a mas and tens of km/sec in kinematics. Two surprising features are: (i) the astrometric effect is of the same order near pericenter as at apocenter, and (ii) the kinematic effect is greatest near (but not at) pericenter.

Newtonian perturbations due to other masses in the Galactic-center region are unknown, but could plausibly be of the same order for the stars so far known. Disentangling the relativistic contribution from the Galactic perturbations may be the hardest problem in practice. It would be necessary to fit simultaneously for post-Newtonian effects and Galactic perturbations, without knowing the specific form of the Galactic perturbation in advance. Whether this is achievable is an open question. Simulations of the modeling pipeline are needed to get a clear answer, but the known and very specific time-dependence of the post-Newtonian effects suggest that we can be optimistic.

We thank the referee, Clifford Will, for confronting some of our numerical results with linear perturbation theory, leading eventually to the comparison with standard post-Newtonian theory that forms Section 5 of the paper.

MP acknowledges support by DLR (Deutsches Zentrum für Luft- und Raumfahrt).

REFERENCES

- Alexander, T. & Hopman, C. 2009, *ApJ*, 697, 1861
- Bahcall, J. & Wolf, R. 1977, *ApJ*, 216, 883
- Blanchet, L. & Iyer, B. R. 2003, *Classical and Quantum Gravity*, 20, 755
- Chandrasekhar, S. 1983, *The mathematical theory of black holes* (Oxford/New York, Clarendon Press/Oxford University Press (International Series of Monographs on Physics. Volume 69), 1983, 663 p.)
- Dexter, J. & Agol, E. 2009, *ArXiv e-prints*, 0903.0620
- Eisenhauer, F., Perrin, G., Brandner, W., Straubmeier, C., Böhm, A., Baumeister, H., Cas-saing, F., Clénet, Y., Dodds-Eden, K., Eckart, A., Gendron, E., Genzel, R., Gillessen, S., Gräter, A., Gueriau, C., Hamaus, N., Haubois, X., Haug, M., Henning, T., Hip-pler, S., Hofmann, R., Hormuth, F., Houairi, K., Kellner, S., Kervella, P., Klein, R., Kolmeder, J., Laun, W., Léna, P., Lenzen, R., Marteau, M., Naranjo, V., Neumann, U., Paumard, T., Rabien, S., Ramos, J. R., Reess, J. M., Rohloff, R.-R., Rouan, D.,

- Rousset, G., Ruyet, B., Sevin, A., Thiel, M., Ziegleder, J., & Ziegler, D. 2009, in *Science with the VLT in the ELT Era*, ed. A. Moorwood, 361–+
- Emel'yanenko, V. V. 2007, *Celestial Mechanics and Dynamical Astronomy*, 98, 191
- Feng, K. 1986, *Journal of Computational Mathematics*, 44, 279
- Forest, E. & Ruth, R. D. 1990, *Physica D: Nonlinear Phenomena*, 43, 105
- Fragile, P. C. & Mathews, G. J. 2000, *ApJ*, 542, 328
- Ghez, A., Salim, S., Weinberg, N., Lu, J., Do, T., Dunn, J., Matthews, K., Morris, M., Yelda, S., Becklin, E., Kremenek, T., Milosavljevic, M., & Naiman, J. 2008, *ApJ*, 689, 1044
- Ghez, A. M., Salim, S., Hornstein, S. D., Tanner, A., Lu, J. R., Morris, M., Becklin, E. E., & Duchêne, G. 2005, *ApJ*, 620, 744
- Gillessen, S., Eisenhauer, F., Trippe, S., Alexander, T., Genzel, R., Martins, F., & Ott, T. 2009, *ApJ*, 692, 1075
- Gürkan, M. A. & Hopman, C. 2007, *MNRAS*, 379, 1083
- Jaroszynski, M. 1998, *Acta Astronomica*, 48, 653
- Kannan, R. & Saha, P. 2009, *ApJ*, 690, 1553
- Kinoshita, H., Yoshida, H., & Nakai, H. 1991, *Celestial Mechanics and Dynamical Astronomy*, 50, 59
- Kraniotis, G. V. 2007, *Classical and Quantum Gravity*, 24, 1775
- Laskar, J. & Robutel, P. 2001, *Celestial Mechanics and Dynamical Astronomy*, 80, 39
- Madigan, A.-M., Levin, Y., & Hopman, C. 2009, *ApJ*, 697, L44
- Mikkola, S. 1997, *Celestial Mechanics and Dynamical Astronomy*, 67, 145
- Mikkola, S. & Aarseth, S. 2002, *Celestial Mechanics and Dynamical Astronomy*, 84, 343
- Mikkola, S. & Merritt, D. 2008, *AJ*, 135, 2398
- Mikkola, S. & Tanikawa, K. 1999, *Celestial Mechanics and Dynamical Astronomy*, 74, 287
- Nucita, A. A., De Paolis, F., Ingrassio, G., Qadir, A., & Zakharov, A. F. 2007, *PASP*, 119, 349

- Perets, H. B., Gualandris, A., Kupi, G., Merritt, D., & Alexander, T. 2009, submitted to ApJ, 99999
- Preto, M. & Amaro-Seoane, P. 2009, to be submitted to ApJ, 99999
- Preto, M. & Tremaine, S. 1999, AJ, 118, 2532
- Rauch, K. & Holman, M. 1999, AJ, 117, 1087
- Saha, P., Stadel, J., & Tremaine, S. 1997, AJ, 114, 409
- Saha, P. & Tremaine, S. 1992, AJ, 104, 1633
- . 1994, AJ, 108, 1962
- Schödel, R., Eckart, A., Alexander, T., Merritt, D., Genzel, R., Sternberg, A., Meyer, L., Kul, F., Moulata, J., Ott, T., & Straubmeier, C. 2007, A&A, 469, 125
- Schödel, R., Merritt, D., & Eckart, A. 2009, arXiv:0902.3892
- Weinberg, N. N., Milosavljević, M., & Ghez, A. M. 2005, ApJ, 622, 878
- Weinberg, S. 1972, Gravitation and Cosmology: Principles and Applications of the General Theory of Relativity (Gravitation and Cosmology: Principles and Applications of the General Theory of Relativity, by Steven Weinberg, pp. 688. ISBN 0-471-92567-5. Wiley-VCH , July 1972.)
- Will, C. M. 2008, ApJ, 674, L25
- Wisdom, J. & Holman, M. 1991, AJ, 102, 1528
- Wisdom, J., Holman, M., & Touma, J. 1996, Fields Institute Communications, Vol. 10, p. 217, 10, 217
- Yoshida, H. 1990, Physics Letters A, 150, 262
- Zucker, S., Alexander, T., Gillessen, S., Eisenhauer, F., & Genzel, R. 2006, ApJ, 639, L21

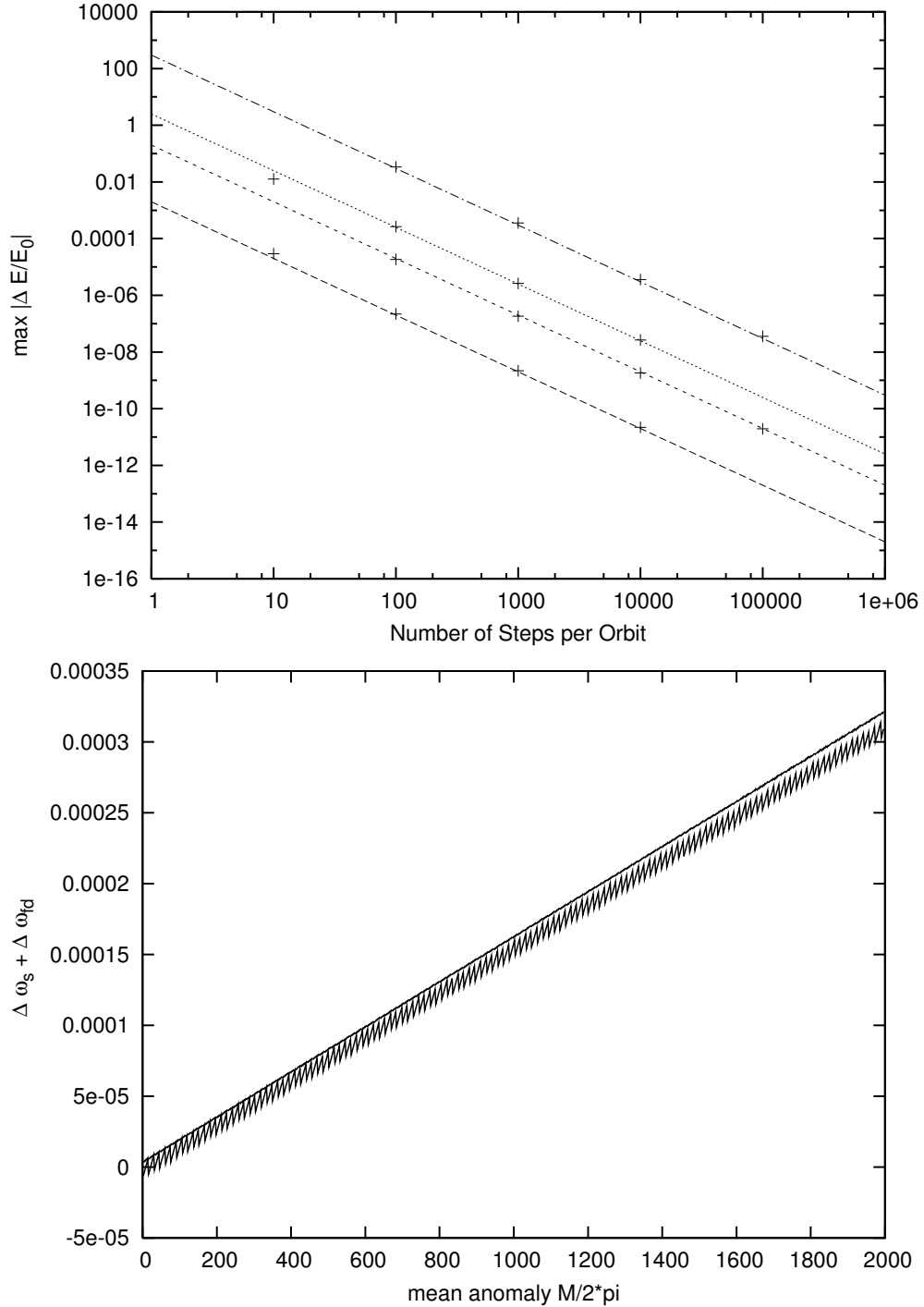


Fig. 1.— Verification of the properties of the integrator. The upper panel shows the maximum error in H over 2000 periods for four orbits with $a = 2.4 \times 10^4$ and $e = 0.5, 0.88, 0.95$ and 0.99 . The lower panel shows the pericenter angle difference between the integration of an S2-like orbit, with initial time steps $1/\Phi(0)$ being 10^{-3} and 10^{-4} of the Keplerian period, and the theoretical value in (29). The oscillations were averaged out from the time series to highlight its (linear) secular evolution, although a small oscillation remains in the former case.

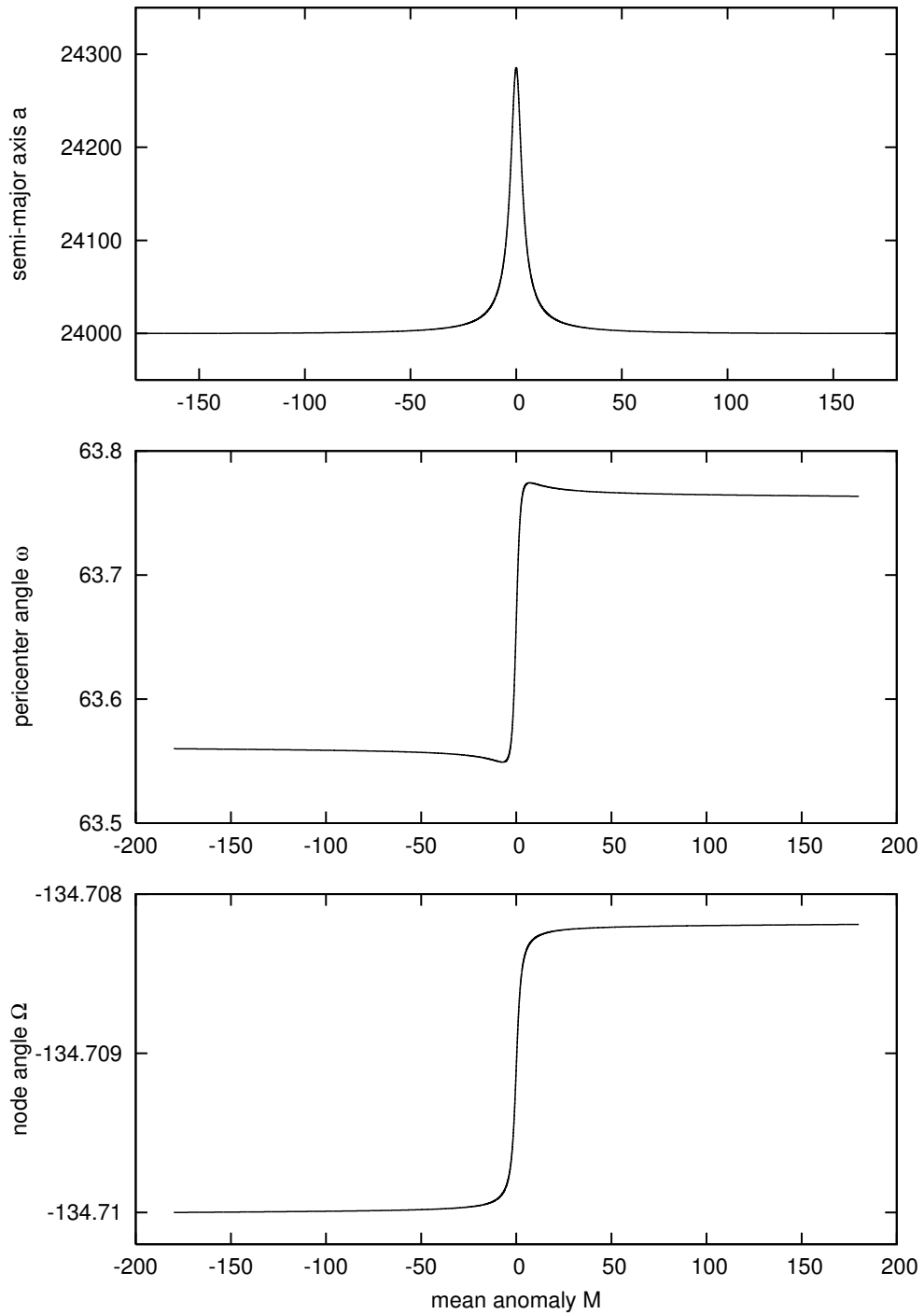


Fig. 2.— Perturbation of the (osculating) orbital elements of an S2-like orbit (see Eq. 28) due to post-Newtonian terms. The upper panel shows a in gravitational units, the middle panel and lower panels show ω and Ω . The mean anomaly is taken as the independent variable, as a surrogate for time (see text). All angles are in degrees.

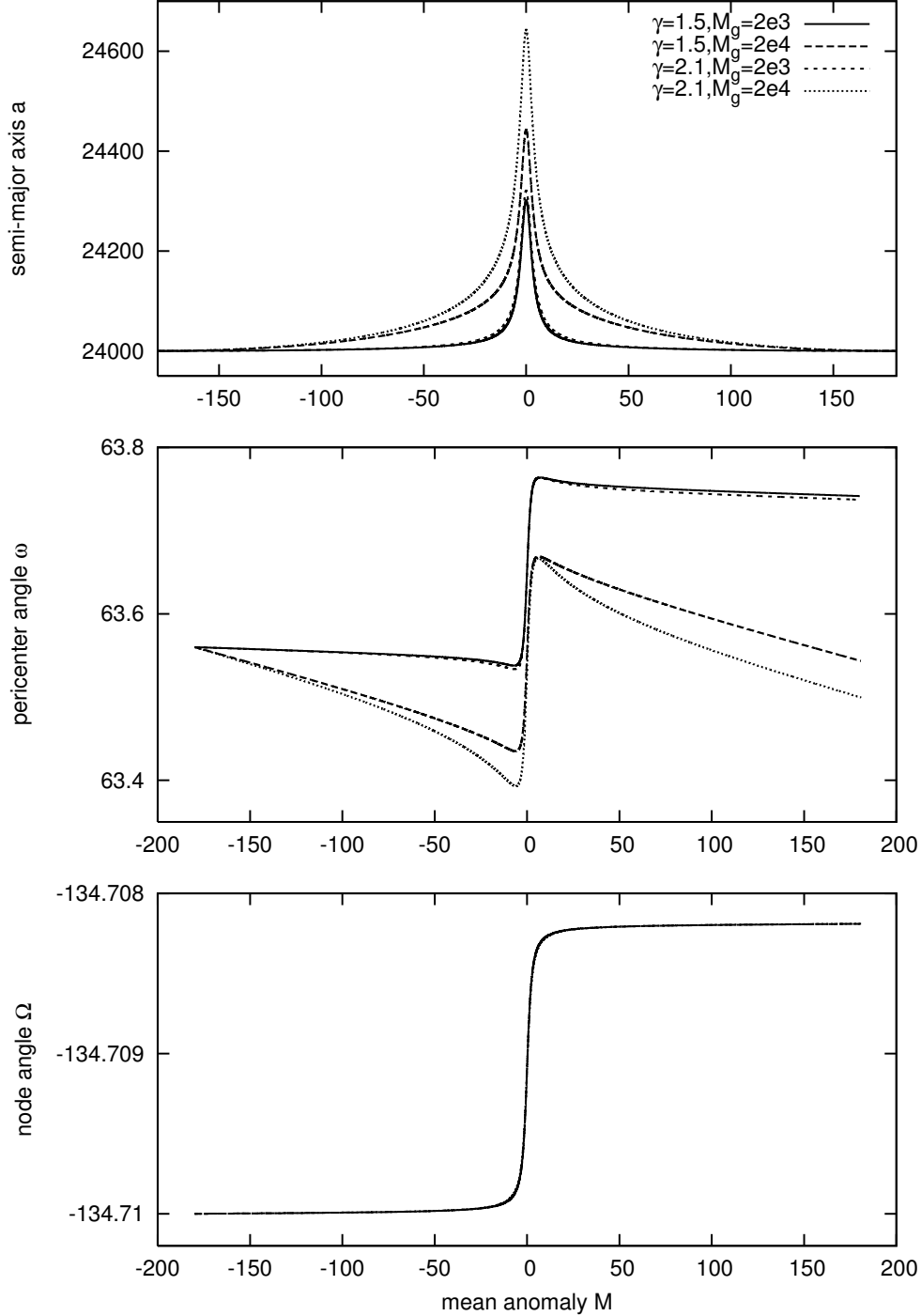


Fig. 3.— Perturbation of the orbital elements of a S2-like orbit due to post-Newtonian terms plus a model for Galactic perturbations consisting of a stellar cluster around Sgr A* (see Eq. 38). The panels are analogous to the two upper panels in Figure 2. For the Galactic contribution, the larger the stellar-cluster and the steeper the cusp, the stronger the perturbation of the elements. The assumed total mass for the stellar cluster is, according to current theoretical estimates, relatively high.

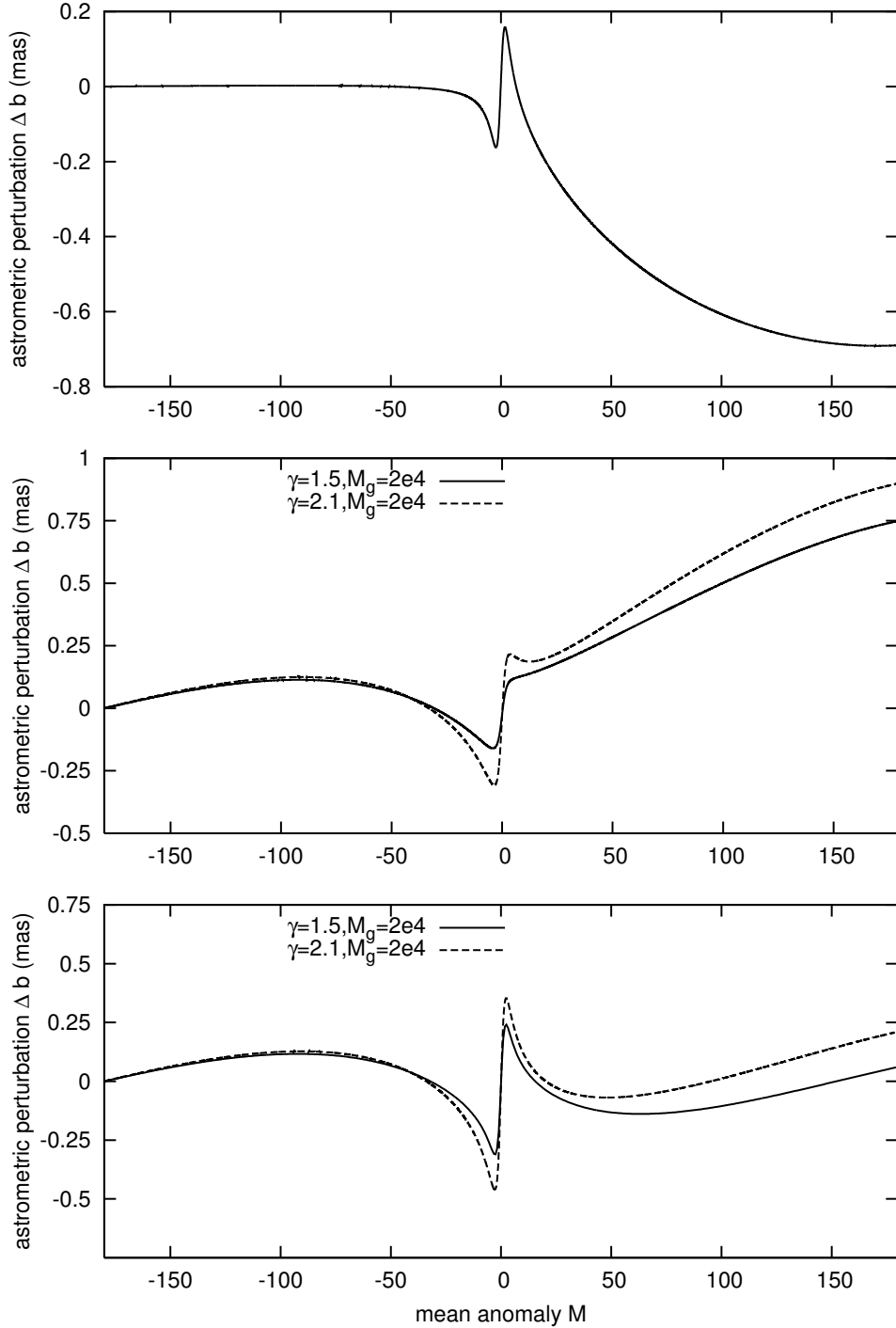


Fig. 4.— Astrometric perturbations for an S2-like orbit. The upper panel shows Δb from post-Newtonian effects only, the middle panel from the model Galactic perturbations only, while the lower panel combines both perturbations. The precession due to both the extended mass distribution and the relativistic effects is too small to be detected with current astrometric capabilities, even though the stellar cusp is relatively massive.

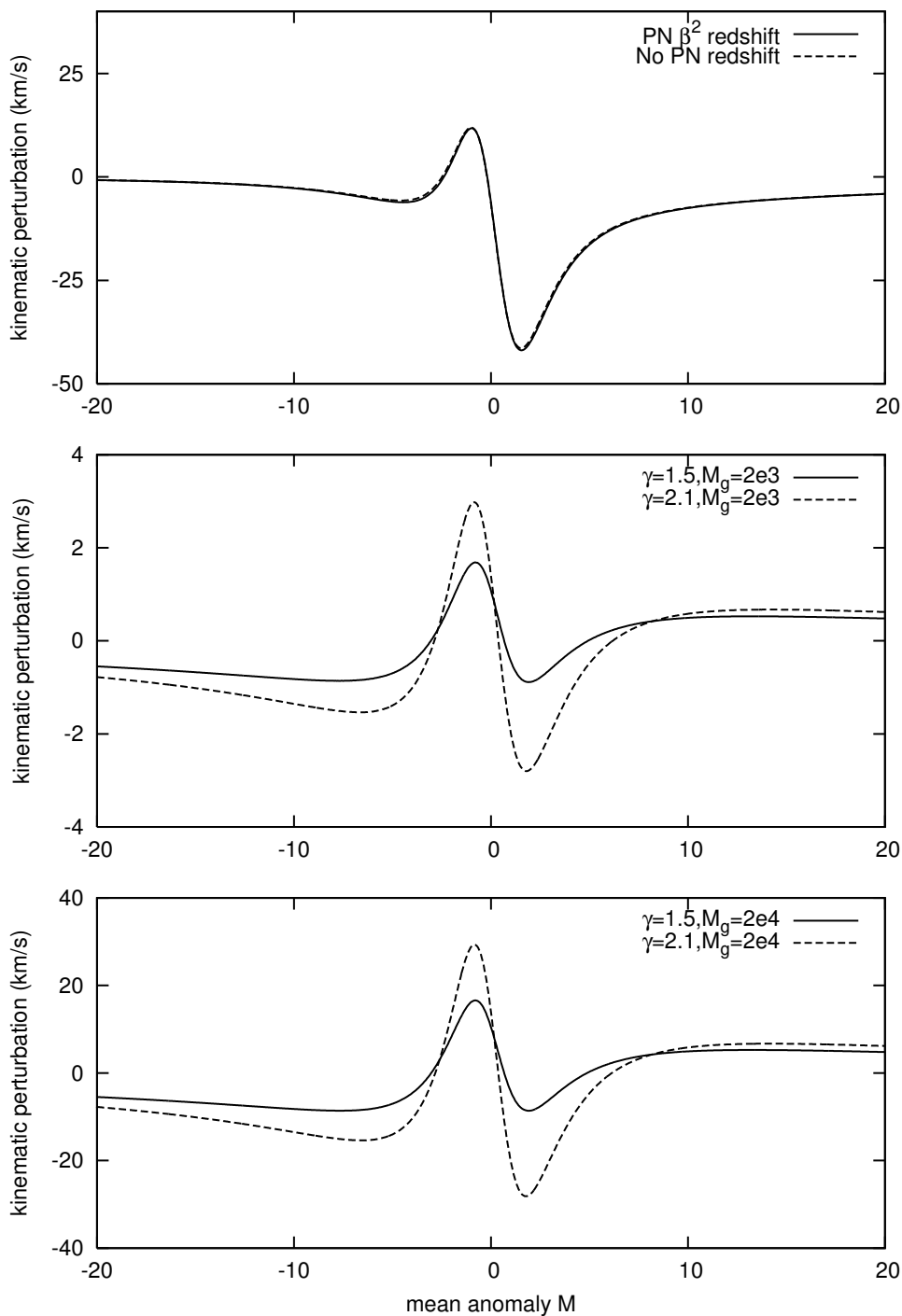


Fig. 5.— Kinematic perturbations. As in Figure 4, the upper panel is from post-Newtonian effects only, the middle panel from the model Galactic perturbations only, and the lower panel combines both. Only the 10% of the orbit around pericenter passage is shown here. The kinematic perturbation due to PN terms on a S2-like orbit appears measurable with current spectroscopic resolution, $\delta v \sim 10$ km/s.

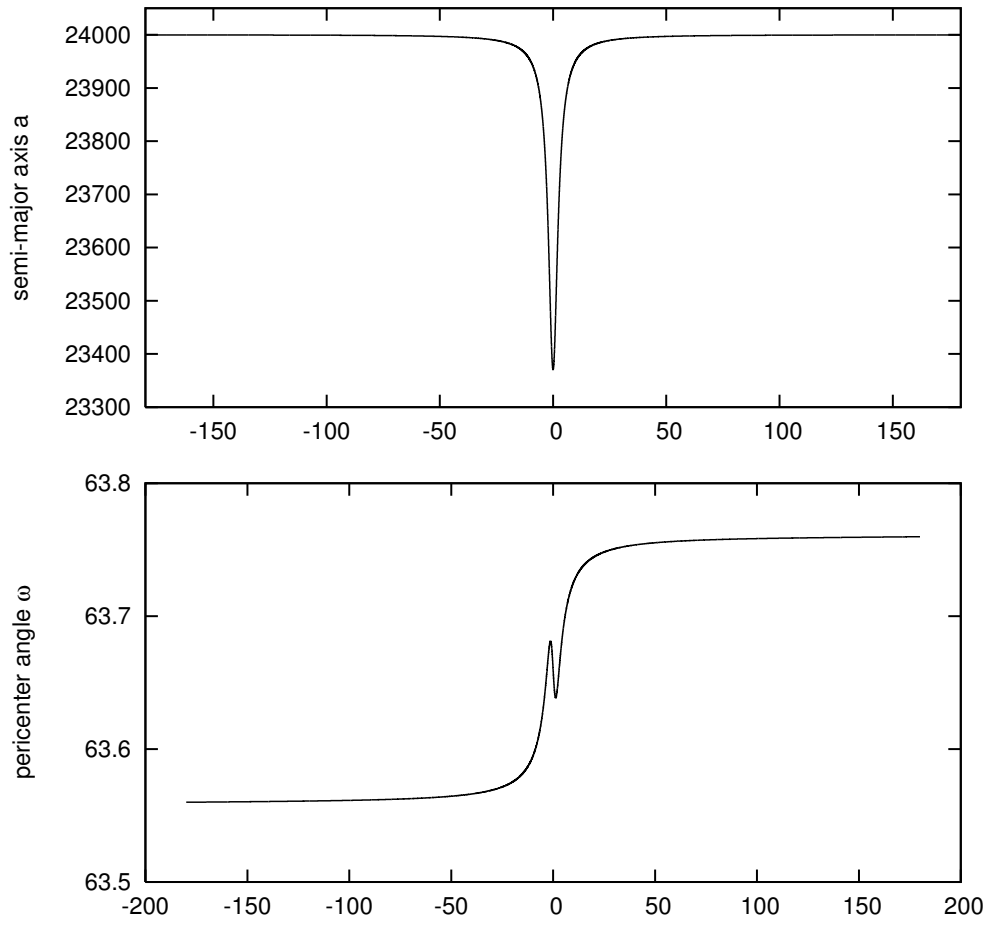


Fig. 6.— Perturbation of the (osculating) orbital elements of an S2-like orbit due to post-Newtonian terms as in Figure 2, but now computing the orbital elements using the “velocity convention”. There are noticeable differences with Figure 2: (i) the perturbation on the semi-major axis changes its sign; (ii) ω now shows a small oscillation around pericenter.